Shell-model study of the $N = 82$ isotonic chain with a realistic effective Hamiltonian

L. Coraggio,[1] A. Covello,[1,2] A. Gargano,[1] N. Itaco,[1,2] and T. T. S. Kuo[3]

[1]*Istituto Nazionale di Fisica Nucleare, Complesso Universitario di Monte S. Angelo, Via Cintia, I-80126 Napoli, Italy*

[2]*Dipartimento di Scienze Fisiche, Università di Napoli Federico II, Complesso Universitario di Monte S. Angelo, Via Cintia, I-80126 Napoli, Italy*

[3]*Department of Physics, SUNY, Stony Brook, New York 11794, USA*

(Received 5 February 2009; revised manuscript received 3 August 2009; published 20 October 2009)

We have performed shell-model calculations for the even- and odd-mass $N = 82$ isotones, focusing attention on low-energy states. The single-particle energies and effective two-body interaction both have been determined within the framework of the time-dependent degenerate linked-diagram perturbation theory, starting from a low-momentum interaction derived from the CD-Bonn nucleon-nucleon potential. In this way, no phenomenological input enters our effective Hamiltonian, whose reliability is evidenced by the good agreement between theory and experiment.

DOI: 10.1103/PhysRevC.80.044320 PACS number(s): 21.60.Cs, 21.30.Fe, 27.60.+j

I. INTRODUCTION

The $N = 82$ region has long been the subject of shell-model studies owing to the strong doubly magic character of ^{132}Sn. In this context, several calculations have been performed employing purely phenomenological two-body effective interactions [1]. Clearly, a main issue in the study of this region is that it provides the opportunity to investigate the effect of adding protons to a doubly magic core over a large number of nuclei (from mass number $A = 133$ to $A = 152$). Comprehensive studies of this kind were conducted some 20 years ago in Refs. [2,3]. In the former a simple pairing Hamiltonian and empirical single-particle (SP) energies were used, while in the latter the two-body matrix elements and single-particle energies were determined simultaneously by a least-squares fit to the ground-state and excited-state energies drawn from all experimentally studied $N = 82$ nuclei.

Starting in the mid-1990s, however, shell-model calculations employing effective interactions derived from realistic nucleon-nucleon (NN) potentials have been performed in the $N = 82$ region, which have generally yielded very good results [4–8]. Some of these studies [5–7] have focused attention on the evolution of the low-energy properties of the $N = 82$ isotones as a function of A, showing that the observed behavior is well reproduced by the theory. In Refs. [6,7] the shell-model results were also compared with those of a quasiparticle random-phase approximation calculation leading to the conclusion that the low-lying states are equally well described by these two approaches.

A main advantage of the above-mentioned realistic shell-model calculations is, of course, that no adjustable parameter appears in the matrix elements of the two-body effective interaction. In all of them, however, the SP energies have been taken from experiment. Actually, the calculational techniques used in these studies are based on the time-dependent degenerate linked-diagram perturbation theory [9], which provides an effective shell-model Hamiltonian, $H_{\rm eff}$, containing both one- and two-body components. Usually, however, the one-body components, which represent the theoretical SP energies, are subtracted from $H_{\rm eff}$ and replaced by those obtained from the experimental spectra of nuclei with one valence nucleon [10]. This procedure has indeed led to a very good description of nuclear properties in different mass regions [11].

Recently, we have performed fully realistic shell-model calculations employing both theoretical SP energies and two-body interactions in studies of p- and sd-shell nuclei [12,13]. In these studies we have renormalized the high-momentum repulsive components of the bare NN potential V_{NN} by way of the so-called $V_{\rm low\text{-}k}$ approach [14,15], which provides a smooth potential preserving exactly the onshell properties of the original V_{NN} up to a cutoff Λ. The effective Hamiltonian has then been derived within the framework of the time-dependent degenerate linked-diagram perturbation theory. In both papers [12,13] a cutoff momentum $\Lambda = 2.1$ fm^{-1} was employed. This corresponds to the laboratory energy $E_{\rm lab} \simeq 350$ MeV, which is the inelastic threshold of the NN scattering. The results of these studies compare well with experiment and other shell-model calculations [16,17].

On these grounds, we have found it interesting to carry out a similar shell-model study of the $N = 82$ chain, focusing attention on the low-lying states of both even- and odd-mass isotones. In this case, the SP energies and two-body effective interaction are determined from a $V_{\rm low\text{-}k}$ derived from the high-precision CD-Bonn potential [18] with a cutoff momentum $\Lambda = 2.6$ fm^{-1}. This value of Λ, which is somewhat larger than that used in our studies of the light nuclei, is needed to obtain a reasonable description of the experimental SP spectrum of the medium-heavy nucleus ^{133}Sb. This is mainly due to the fact that, at variance with the model spaces for light nuclei, in this case the 50–82 major shell contains the intruder $0h_{11/2}$ state, whose relative energy turns out to be strongly sensitive to the value of Λ. More precisely, for small values of Λ this state lies far away from the other SP levels of the 50–82 shell, while the correct structure of this shell is restored when increasing the value of Λ [19].

The dependence of the results on Λ would obviously vanish when complementing the $V_{\rm low\text{-}k}$ effective two-body interaction with different three- and higher-body components for each value of Λ. However, it is at present a very hard task, from the computational point of view, to take into account

two- and three-body forces on an equal footing in a third-order perturbative calculation for medium- and heavy-mass nuclei. Therefore, the value of the cutoff Λ may be considered as a parameter that we have chosen to reproduce satisfactorily the experimental SP spectrum. For the sake of completeness, it should be mentioned that the trend of our calculated SP energies suggests that a larger value of the cutoff could even improve the agreement with experiment. However, this would amount to include higher-momentum components, which would rapidly deteriorate the convergence properties of the perturbative expansion used to derive the effective shell-model Hamiltonian. In the following section we show that our choice of Λ is a reasonable compromise to assure both good perturbative properties and quality of the results.

The article is organized as follows. In Sec. II we give a brief outline of our calculations, focusing attention on the convergence properties of the effective Hamiltonian. Section III is devoted to the presentation and discussion of our results, while some concluding remarks are given in Sec. IV.

II. OUTLINE OF CALCULATIONS

Our goal is to derive an effective Hamiltonian for shell-model calculations in the proton $2s1d0g0h$ shell, which is the standard model space to describe the spectroscopic properties of $N = 82$ isotones. Within the framework of the shell model, an auxiliary one-body potential U is introduced to break up the Hamiltonian for a system of A nucleons as the sum of a one-body term H_0, which describes the independent motion of the nucleons, and a residual interaction H_1:

$$H = \sum_{i=1}^{A} \frac{p_i^2}{2m} + \sum_{i<j=1}^{A} V_{ij}^{NN} = T + V = (T + U) + (V - U) = H_0 + H_1. \quad (1)$$

Once H_0 has been introduced, a reduced model space is defined in terms of a finite subset of H_0's eigenvectors. The diagonalization of the many-body Hamiltonian (1) in an infinite Hilbert space, that it is obviously unfeasible, is then reduced to the solution of an eigenvalue problem for an effective Hamiltonian H_{eff} in a finite space.

In this article, we derive H_{eff} by way of the time-dependent perturbation theory [9]. Namely, H_{eff} is expressed through the Kuo-Lee-Ratcliff (KLR) folded-diagram expansion in terms of the vertex function $\hat{Q}$-box, which is composed of irreducible valence-linked diagrams [20,21]. We include in the $\hat{Q}$-box one- and two-body Goldstone diagrams through third order in H_1. The folded-diagram series is summed up to all orders using the Lee-Suzuki iteration method [22].

The Hamiltonian H_{eff} contains one-body contributions, whose collection is the so-called $\hat{S}$-box [10]. As mentioned in the Introduction, in realistic shell-model calculations it is customary to use a subtraction procedure so only the two-body terms of H_{eff}, which make up the effective interaction V_{eff}, are retained while the SP energies are taken from experiment. In this work, we have adopted a different approach, employing SP energies obtained from the $\hat{S}$-box calculation. In this regard, it is worth pointing out that, due to the presence of the $-U$ term in H_1, U-insertion diagrams arise in the $\hat{Q}$-box. In our calculation we use the harmonic oscillator (HO) potential, $U = \frac{1}{2}m\omega^2 r^2$, and take into account all U-insertion diagrams up to third order. The oscillator parameter is $\hbar\omega = 7.88$ MeV, according to the expression [23] $\hbar\omega = 45A^{-1/3} - 25A^{-2/3}$ for $A = 132$.

Let us now outline the $V_{\text{low-k}}$ approach [14,15] to the renormalization of V_{NN}. The repulsive core contained in V_{NN} is smoothed by integrating out the high-momentum modes of V_{NN} down to a certain cutoff Λ. This integration is carried out with the requirement that the deuteron binding energy and phase shifts of V_{NN} are preserved by $V_{\text{low-k}}$, which is achieved by the following T-matrix equivalence approach. We start from the half-on-shell T matrix for V_{NN}

$$T(k', k, k^2) = V_{NN}(k', k) + \mathcal{P}\int_0^\infty q^2 dq\, V_{NN}(k', q) \times \frac{1}{k^2 - q^2} T(q, k, k^2), \quad (2)$$

where $\mathcal{P}$ denotes the principal value and k, k', and q stand for the relative momenta. The effective low-momentum T matrix is then defined by

$$T_{\text{low-k}}(p', p, p^2) = V_{\text{low-k}}(p', p) + \mathcal{P}\int_0^\Lambda q^2 dq\, V_{\text{low-k}}(p', q) \times \frac{1}{p^2 - q^2} T_{\text{low-k}}(q, p, p^2), \quad (3)$$

where the intermediate state momentum q is integrated from 0 to the momentum space cutoff Λ and $(p', p) \leqslant \Lambda$. The above T matrices are required to satisfy the condition

$$T(p', p, p^2) = T_{\text{low-k}}(p', p, p^2); (p', p) \leqslant \Lambda. \quad (4)$$

The above equations define the effective low-momentum interaction $V_{\text{low-k}}$, and it has been shown [15] that their solution is provided by the KLR folded-diagram expansion [9,20] mentioned before. In addition to the preservation of the half-on-shell T matrix, which implies preservation of the phase shifts, this $V_{\text{low-k}}$ preserves the deuteron binding energy, because eigenvalues are preserved by the KLR effective interaction. For any value of Λ, the $V_{\text{low-k}}$ can be calculated very accurately using iteration methods. Our calculation of $V_{\text{low-k}}$ is performed by employing the method proposed in Ref. [24], which is based on the Lee-Suzuki similarity transformation [22].

As mentioned in the Introduction, our $V_{\text{low-k}}$ has been derived from the CD-Bonn NN potential with a cutoff momentum $\Lambda = 2.6$ fm^{-1}, and for protons the Coulomb force has been explicitly added to $V_{\text{low-k}}$.

A discussion of the convergence properties of H_{eff} is now in order. For the sake of clarity, we first consider the two-body matrix elements (TBME) of V_{eff} and then the SP energies.

In Fig. 1, we report the diagonal $J^\pi = 0^+$ TBME of V_{eff} as a function of the maximum allowed excitation energy of the intermediate states expressed in terms of the oscillator quanta $N_{\max}$. We have chosen the $J^\pi = 0^+$ matrix elements because they are the largest ones in the entire set of V_{eff} TBME and play a key role in determining the relative spectra and ground-state

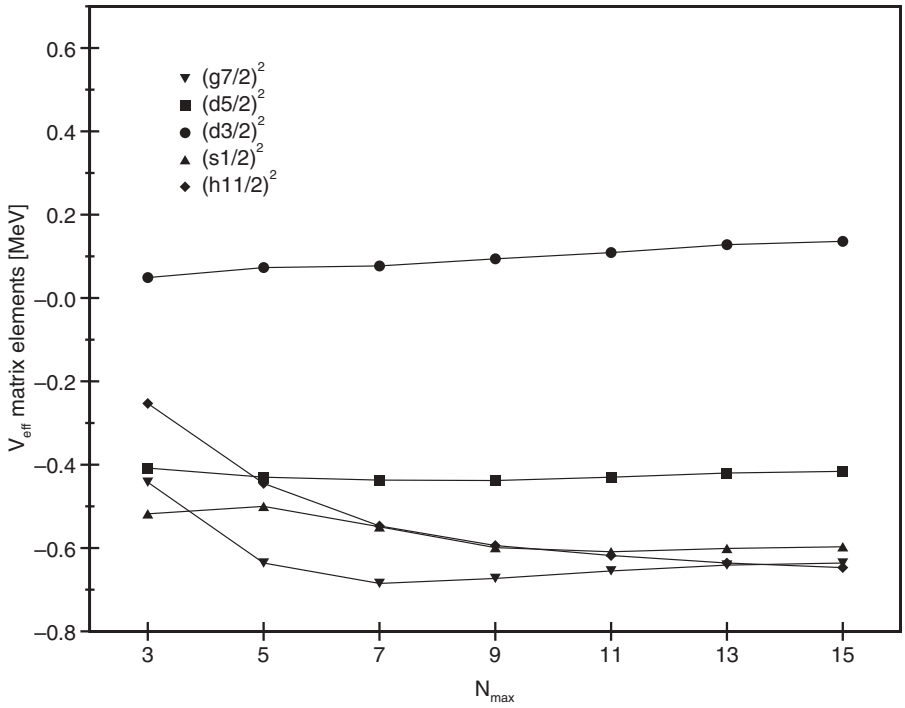

FIG. 1. Diagonal $J^\pi = 0^+$ TBME of V_{eff} as a function of $N_{\max}$ (see text for details).

(g.s.) properties of the even $N = 82$ isotones. From Fig. 1 it is clear that our results have practically achieved convergence at $N_{\max} = 15$.

As regards the order-by-order convergence, an estimate of the value to which the perturbative series should converge may be obtained by using Padé approximants. In Table I, we compare all the $\hat{Q}$-box $J^\pi = 0^+$ TBME calculated at third order with those given by the [2|1] Padé approximant [25]

$$[2|1] = V^0_{Q\text{-box}} + V^1_{Q\text{-box}} + \frac{V^2_{Q\text{-box}}}{1 - V^3_{Q\text{-box}}/V^2_{Q\text{-box}}}, \qquad (5)$$

TABLE I. $\hat{Q}$-box $J^\pi = 0^+$ two-body matrix elements at third order in $V_{\text{low-k}}$ (in MeV) compared with those obtained by calculating the Padé approximant [2|1].

Configuration	Third order	Padé [2|1]
$\langle(0g_{7/2})^2\|V_{Q\text{-box}}\|(0g_{7/2})^2\rangle$	−0.8624	−0.8757
$\langle(0g_{7/2})^2\|V_{Q\text{-box}}\|(1d_{5/2})^2\rangle$	−1.0022	−1.0196
$\langle(0g_{7/2})^2\|V_{Q\text{-box}}\|(1d_{3/2})^2\rangle$	−0.6948	−0.6999
$\langle(0g_{7/2})^2\|V_{Q\text{-box}}\|(2s_{1/2})^2\rangle$	−0.4642	−0.4662
$\langle(0g_{7/2})^2\|V_{Q\text{-box}}\|(0h_{11/2})^2\rangle$	2.0532	2.0580
$\langle(1d_{5/2})^2\|V_{Q\text{-box}}\|(1d_{5/2})^2\rangle$	−0.7069	−0.7138
$\langle(1d_{5/2})^2\|V_{Q\text{-box}}\|(1d_{3/2})^2\rangle$	−1.7611	−1.8191
$\langle(1d_{5/2})^2\|V_{Q\text{-box}}\|(2s_{1/2})^2\rangle$	−0.6807	−0.7555
$\langle(1d_{5/2})^2\|V_{Q\text{-box}}\|(0h_{11/2})^2\rangle$	1.2028	1.2081
$\langle(1d_{3/2})^2\|V_{Q\text{-box}}\|(1d_{3/2})^2\rangle$	0.0838	0.0447
$\langle(1d_{3/2})^2\|V_{Q\text{-box}}\|(2s_{1/2})^2\rangle$	−0.4817	−0.4857
$\langle(1d_{3/2})^2\|V_{Q\text{-box}}\|(0h_{11/2})^2\rangle$	1.0457	1.0459
$\langle(2s_{1/2})^2\|V_{Q\text{-box}}\|(2s_{1/2})^2\rangle$	−0.8820	−0.4686
$\langle(2s_{1/2})^2\|V_{Q\text{-box}}\|(0h_{11/2})^2\rangle$	0.6580	0.6586
$\langle(0h_{11/2})^2\|V_{Q\text{-box}}\|(0h_{11/2})^2\rangle$	−0.8025	−0.8391

$V^n_{Q\text{-box}}$ being the nth-order contribution to the $J^\pi = 0^+$ TBME in the linked-diagram expansion. From Table I we see that our third-order results are in good agreement with those from the [2|1] Padé approximant, the differences being all in the order of few tens of keV with the exception of the diagonal matrix element for the $(2s_{1/2})^2$ configuration. This indicates a weak dependence of our results on higher-order $\hat{Q}$-box perturbative terms.

In Fig. 2 we report the relative SP energies calculated at third order in H_1 as a function of $N_{\max}$. In the same figure, the results

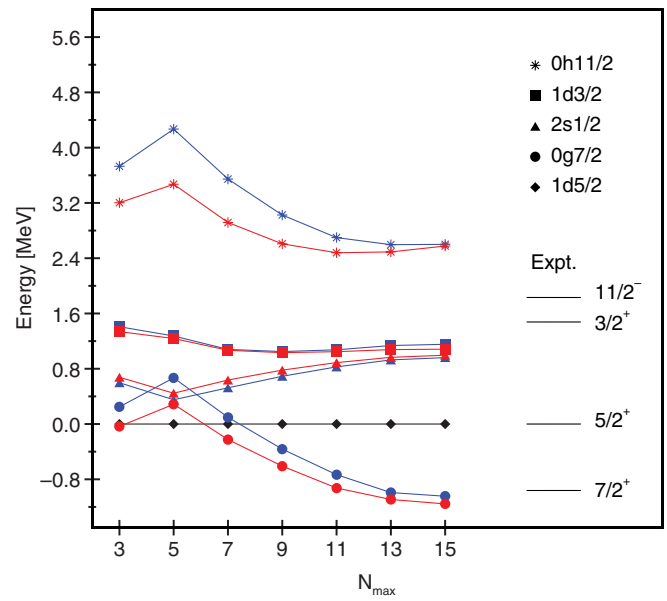

FIG. 2. (Color online) Theoretical relative SP energies as a function of $N_{\max}$ (see text for details). The experimental spectrum of ^{133}Sb is also reported.

obtained by calculating the Padé approximant [2|1] are also reported (red lines). Once again, the agreement between third-order results and those from this approximant points to a good perturbative behavior of the calculated relative SP energies. We also see that an $N_{\max} = 15$ calculation yields satisfactorily converged values for the relative SP energies.

A different situation occurs for the absolute SP energies. Actually, the calculated energy of the $1d_{5/2}$ level relative to ^{132}Sn is -4.468, -5.225, and -5.954 MeV for ($N_{\max} = 11$, 13, and 15, respectively. This shows that there is no sign of convergence of the absolute SP energies as a function of the number of intermediate states. Moreover, the Padé approximant [2|1] of the $1d_{5/2}$ energy for $N_{\max} = 15$ is equal to -7.262, showing that also the order-by-order convergence of the absolute SP energies is unsatisfactory. This poor perturbative behavior may be traced to the chosen value of the cutoff momentum, $\Lambda = 2.6$ fm^{-1}, which is substantially larger than the standard one, $\Lambda \simeq 2.1$ fm^{-1}. However, the inaccuracy of the absolute SP energies affects only the ground-state energies of the nuclei considered. In fact, the calculated spectroscopic properties (energy spectra, electromagnetic transition rates) are certainly reliable, based on the good convergence of the relative SP energies and TBME.

III. RESULTS AND DISCUSSION

We have performed calculations, using the OSLO shell-model code [26], for the even-mass $N = 82$ isotones up to ^{154}Hf, which is the last known nucleus belonging to this chain, and for the odd-mass ones up to ^{149}Ho, the last odd-mass nucleus with a well-established experimental low-lying energy spectrum. This is the longest isotonic chain approaching the proton drip line and therefore provides an interesting laboratory to study the evolution of nuclear structure when adding pairs of identical particles.

In Table II our calculated SP energies are reported and compared with the experimental spectrum of ^{133}Sb. We see that the latter is on the whole reasonably well reproduced by the theory. However, while the calculated positions of the $1d_{5/2}$ and $1d_{3/2}$ levels come very close to the experimental ones, the energy of the $0h_{11/2}$ level is overestimated by about 0.85 MeV. As we shall discuss later in this section, the energy of the $2s_{1/2}$ level, for which there is no experimental information, appears to be somewhat underestimated.

TABLE II. Calculated SP relative energies (in MeV), compared with the experimental spectrum of ^{133}Sb [27]. The values in parenthesis are the absolute SP energies with respect to the doubly closed ^{132}Sn.

nlj	Calc.	Expt.
$0g_{7/2}$	0.000 (-6.999)	0.000 (-9.663)
$1d_{5/2}$	1.045	0.962
$1d_{3/2}$	2.200	2.440
$2s_{1/2}$	2.006	
$0h_{11/2}$	3.645	2.793

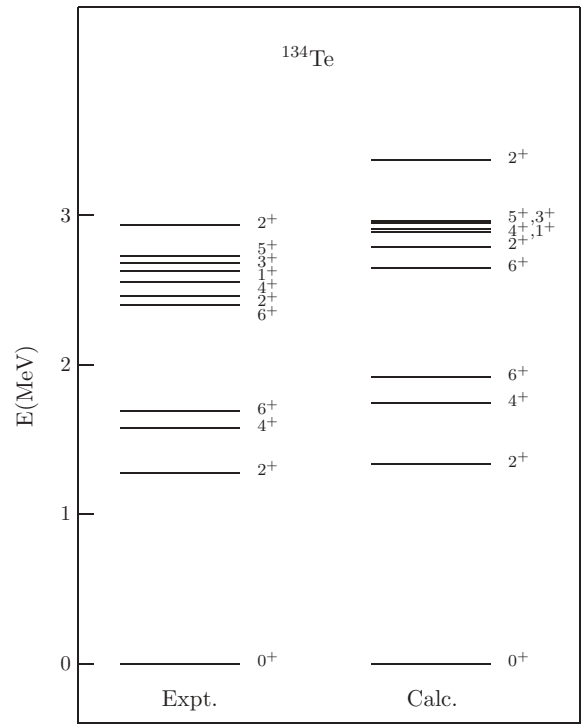

FIG. 3. Experimental and calculated ^{134}Te spectra.

A strong test for our effective Hamiltonian is given by the calculation of the energy spectrum of ^{134}Te, because the theory of the effective interaction is tailored for systems with two valence nucleons. From Fig. 3, where the experimental [27] and calculated ^{134}Te spectra are reported up to 3.5 MeV excitation energy, we see that a very good agreement is indeed obtained.

In Fig. 4, we show the calculated and experimental [28] ground-state energies (relative to the ^{132}Sn core) per valence proton as a function of the number of valence particles Z_{val} of even-mass isotopes. We see that the experimental and theoretical curves are practically straight lines having the same slope, while being about 2.4 MeV apart. This discrepancy is essentially the same as that existing between the theoretical and experimental ground-state energies of ^{133}Sb (see Table II). This confirms the reliability of our SP spacings and TBME, because the pattern of the theoretical curve depends only on these quantities.

In Figs. 5, 6, and 7 we report, as a function of the mass number A, the experimental and calculated excitation energies of the 2^+, 4^+, and 6^+ yrast states, respectively. The experimental behavior is well reproduced, expecially for the $J^\pi = 2^+$ and 4^+ states, for which the discrepancies do not exceed 350 keV. However, it should be noted that according to our calculations the proton subshell closure, which experimentally occurs at ^{146}Gd, is not reproduced. As mentioned before, this can be traced to the theoretical position of the $2s_{1/2}$ orbital, which appears to be too low in energy. This is confirmed by the fact [4] that this level has to be placed at 2.8 MeV to reproduce the experimental energy of the $J^\pi = \frac{1}{2}^+$ at 2.150 MeV in ^{137}Cs, which is predominantly of SP nature [29]. We have verified that, if the $2s_{1/2}$ SP level

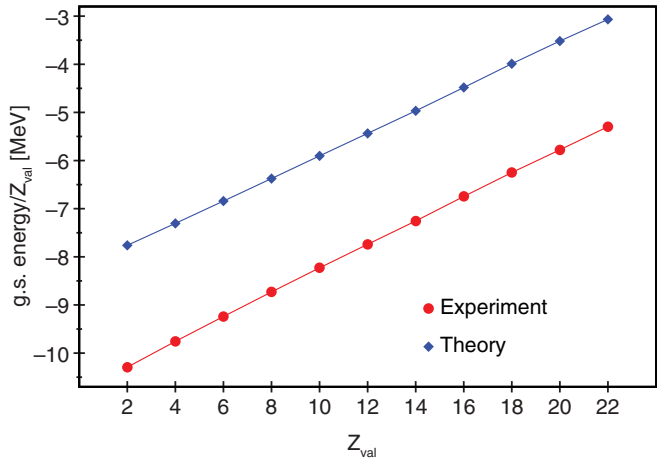

FIG. 4. (Color online) Experimental and calculated ground-state energies per valence proton for $N = 82$ isotones from $A = 134$ to 154. Z_{val} is the number of valence protons.

is placed at 2.8 MeV, we obtain that the 2_1^+ excitation energy in ^{146}Gd raises from 1.716 MeV to 1.976 MeV, while in ^{148}Dy it decreases from 1.827 to 1.758 MeV, thus reproducing the observed subshell closure.

To have a more complete test of the theory, we have also calculated the $B(E2; 2_1^+ \to 0_1^+)$ transition rates up to ^{144}Sm, employing an effective operator obtained at third order in perturbation theory, consistently with the derivation of H_{eff}. Our results are reported and compared with the experimental data in Table III Ref. [27]. We see that the agreement is quite good, providing evidence for the reliability of our calculated effective operator that takes into account microscopically core-polarization effects.

Let us now come to the odd-mass isotones. In Figs. 8–11 we report, as a function of the mass number A, the experimental and calculated energies of the $\frac{5}{2}^+$, $\frac{3}{2}^+$, $\frac{1}{2}^+$, and $\frac{11}{2}^-$ yrast states relative to the $\frac{7}{2}^+$ yrast state, respectively. The experimental behavior is well reproduced for the $\frac{5}{2}^+$, $\frac{3}{2}^+$, and $\frac{11}{2}^-$ states. For the latter, however, most of the calculated energies are higher than the experimental ones by about 300–400 keV, which reflects the theoretical overestimation of the value of

TABLE III. Experimental and calculated $B(E2; 2_1^+ \to 0_1^+)$. The reduced transition probabilities are expressed in W.u..

Nucleus	Calc.	Expt.
^{134}Te	5.5	6.3 ± 2.0
^{136}Xe	9.06	16.6 ± 2.4
^{138}Ba	11.1	10.8 ± 0.5
^{140}Ce	14.5	13.8 ± 0.3
^{142}Nd	16.26	12.03 ± 0.22
^{144}Sm	16.6	11.9 ± 0.4

the $0h_{11/2}$ SP energy. Less satisfactory is the comparison between the calculated and experimental behavior of the $\frac{1}{2}^+$ yrast states, which is a further confirmation that the theoretical $2s_{1/2}$ level in ^{133}Sb lies too low in energy. As a matter of fact, by performing a calculation within the seniority scheme up to $v = 3$, we have found that in ^{137}Cs and ^{139}La the lowest $\frac{1}{2}^+$ states, which are quite well reproduced by the theory, have significant seniority $v = 3$ components. From $A = 141$ onward, the experimental $(\frac{1}{2}^+)_1$ levels are predominantly of SP nature, as confirmed by the spectroscopic factors [27], and the corresponding calculated states, which are dominated by $v = 1$ components, underestimate their energies.

As pointed out in the Introduction, the main purpose of this study has been to test the use of a fully realistic shell-model Hamiltonian for the description of medium-heavy mass nuclei. In this context, it should be noted that, aside from adopting experimental single-particle energies, earlier calculations on the $N = 82$ isotones differ from the present ones in other respects, like the starting NN potential and the renormalization procedure. For instance, while we employ the CD-Bonn potential renormalized through the $V_{\text{low-k}}$ procedure, in the works of Refs. [6,7] use is made of the Bonn-A potential and the Brueckner G-matrix approach. A comparison between the results of earlier works and the present one would not therefore be very meaningful. It is worth mentioning, however, that the agreement between experiment and theory achieved in this article is on the whole comparable with that obtained

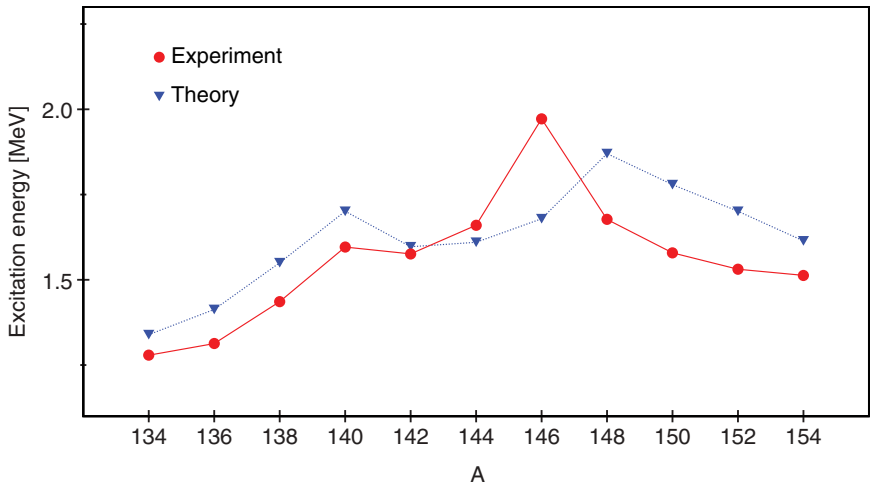

FIG. 5. (Color online) Experimental and calculated excitation energies of the yrast $J^\pi = 2^+$ states for $N = 82$ isotones.

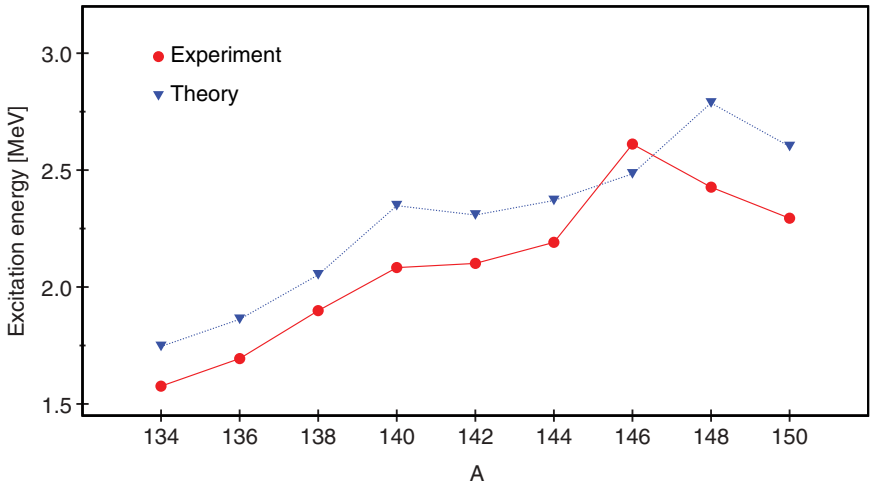

FIG. 6. (Color online) Experimental and calculated excitation energies of the yrast $J^\pi = 4^+$ states for $N = 82$ isotones.

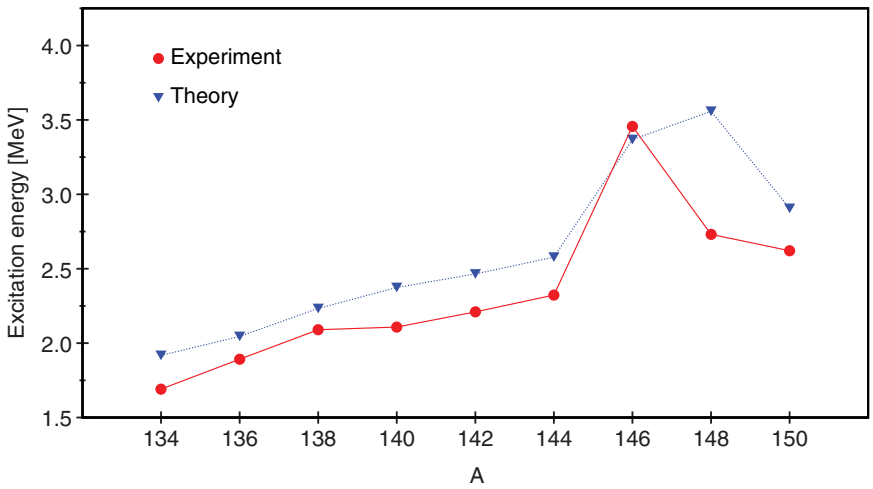

FIG. 7. (Color online) Experimental and calculated excitation energies of the yrast $J^\pi = 6^+$ states for $N = 82$ isotones.

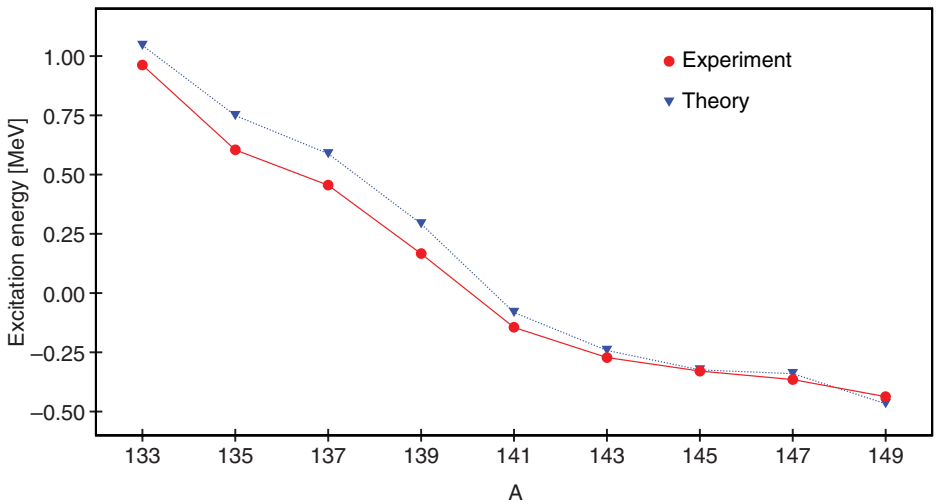

FIG. 8. (Color online) Experimental and calculated energies of the yrast $J^\pi = \frac{5}{2}^+$ states relative to $J^\pi = (\frac{7}{2}^+)_1$ for odd-mass $N = 82$ isotones.

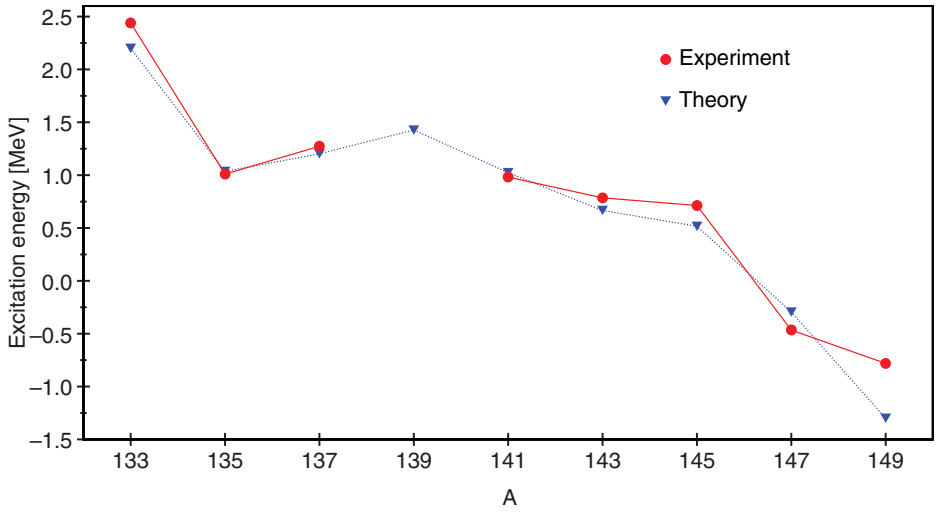

FIG. 9. (Color online) Experimental and calculated energies of the yrast $J^\pi = \frac{3}{2}^+$ states relative to $J^\pi = (\frac{7}{2}^+)_1$ for odd-mass $N = 82$ isotones.

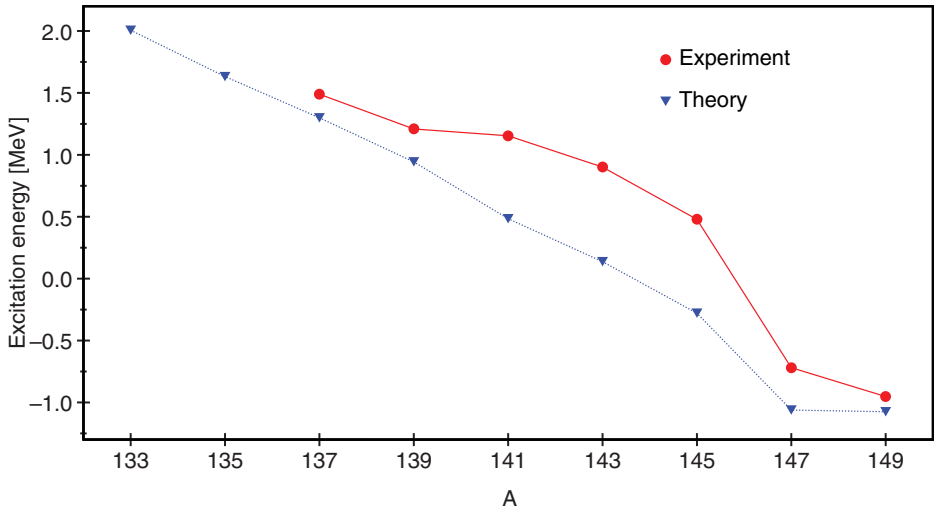

FIG. 10. (Color online) Experimental and calculated energies of the yrast $J^\pi = \frac{1}{2}^+$ states relative to $J^\pi = (\frac{7}{2}^+)_1$ for odd-mass $N = 82$ isotones.

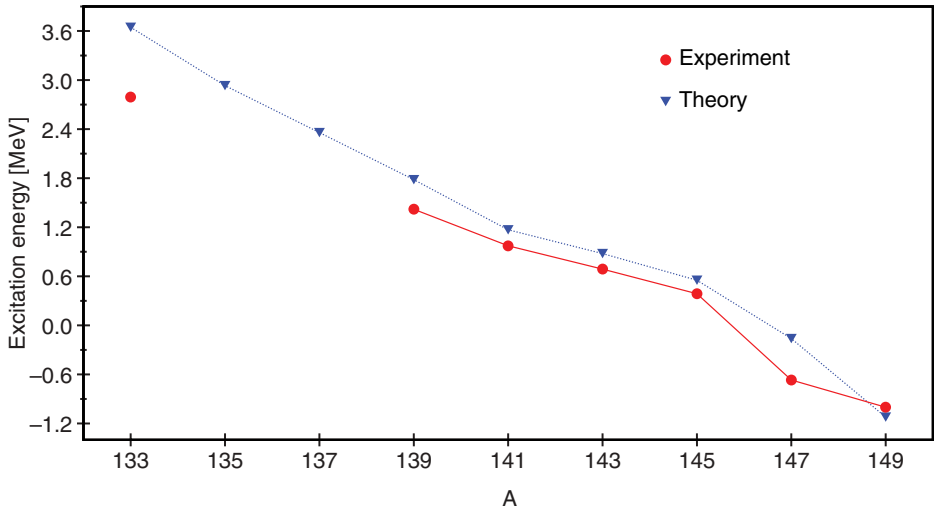

FIG. 11. (Color online) Experimental and calculated energies of the yrast $J^\pi = \frac{11}{2}^-$ states relative to $J^\pi = (\frac{7}{2}^+)_1$ for odd-mass $N = 82$ isotones.

in the previous calculations employing realistic effective interactions.

IV. CONCLUDING REMARKS

As discussed in detail in the Introduction, the $N = 82$ isotonic chain has long been considered a benchmark for shell-model calculations. This has resulted in a number of theoretical works that have practically all led to a good description of low-energy properties of these nuclei, evidencing the strong doubly magic character of ^{132}Sn.

A main step toward a microscopic shell-model description of nuclear structure has been the use of two-body effective interactions derived from the free nucleon-nucleon potential. This approach, in which no adjustable parameter is involved in the calculation of the TBME, has been successfully applied to the $N = 82$ isotones in the past decade, showing the ability of realistic effective interactions to provide an accurate description of nuclear structure properties.

However, some important theoretical questions still remain open. In particular, these concern the calculation of the single-particle energies and the role of three-body correlations. In the present article, we have tried to investigate the former issue by constructing a realistic effective shell-model Hamiltonian for the $N = 82$ isotones, where both the SP energies and TBME have been obtained starting from a $V_{\text{low-k}}$ derived from the CD-Bonn potential. This is a natural extension of our studies of p-shell nuclei [12] and oxygen isotopes [13]. Here, we have shown that our effective Hamiltonian yields results that are in quite good agreement with experiment along the whole chain of the $N = 82$ isotones. As regards the calculated single-particle energies, significant discrepancies with the experimental values occur only for the $0h_{11/2}$ and $2s_{1/2}$ levels. Note that for the latter no direct comparison is possible because the single-particle $2s_{1/2}$ state is still missing in the experimental spectrum of ^{133}Sb. However, we have verified that increasing the calculated value by 0.8 MeV the proton subshell closure occurs at ^{146}Gd, in agreement with the experimental findings.

At this point, the question naturally arises as to how contributions from three-body forces would modify the present results, in particular as regards the single-particle energies. While this remains a major task for future investigation, we feel that the present study paves the way toward a better understanding of the microscopic foundations of the nuclear shell model.

ACKNOWLEDGMENT

This work was supported in part by the US DOE Grant No. DE-FG02-88ER40388.

[1] S. Sarkar and M. S. Sarkar, Phys. Rev. C **64**, 014312 (2001), and references therein.
[2] F. Andreozzi, A. Covello, A. Gargano, and A. Porrino, Phys. Rev. C **41**, 250 (1990).
[3] B. H. Wildenthal, in *Understanding the Variety of Nuclear Excitations: Proceedings of the 3rd International Spring Seminar on Nuclear Physics, Ischia, 1990*, edited by A. Covello (World Scientific, Singapore, 1991), p. 35.
[4] F. Andreozzi, L. Coraggio, A. Covello, A. Gargano, T. T. S. Kuo, and A. Porrino, Phys. Rev. C **56**, R16 (1997).
[5] A. Covello, F. Andreozzi, L. Coraggio, A. Covello, A. Gargano, T. T. S. Kuo, and A. Porrino, Prog. Part. Nucl. Phys. **38**, 165 (1997).
[6] A. Holt, T. Engeland, E. Osnes, M. Hjorth-Jensen, and J. Suhonen, Nucl. Phys. **A618**, 107 (1997).
[7] J. Suhonen, J. Toivanen, A. Holt, T. Engeland, E. Osnes, and M. Hjorth-Jensen, Nucl. Phys. **A628**, 41 (1998).
[8] A. Covello, L. Coraggio, A. Gargano, N. Itaco, and T. T. S. Kuo, in *Challenges in Nuclear Sructure: Proceedings of the 7th International Spring Seminar on Nuclear Physics, Maiori, 2001*, edited by A. Covello (World Scientific, Singapore, 2002), p. 139.
[9] T. T. S. Kuo and E. Osnes, *Folded-Diagram Theory of the Effective Interaction in Nuclei, Atoms and Molecules, Lecture Notes in Physics* (Springer-Verlag, Berlin, 1990), Vol. 364.
[10] J. Shurpin, T. T. S. Kuo, and D. Strottman, Nucl. Phys. **A408**, 310 (1983).
[11] L. Coraggio, A. Covello, A. Gargano, N. Itaco, and T. T. S. Kuo, Prog. Part. Nucl. Phys. **62**, 135 (2009).
[12] L. Coraggio and N. Itaco, Phys. Lett. **B616**, 43 (2005).
[13] L. Coraggio, A. Covello, A. Gargano, N. Itaco, D. R. Entem, T. T. S. Kuo, and R. Machleidt, Phys. Rev. C **75**, 024311 (2007).
[14] S. Bogner, T. T. S. Kuo, and L. Coraggio, Nucl. Phys. **A684**, 432c (2001).
[15] S. Bogner, T. T. S. Kuo, L. Coraggio, A. Covello, and N. Itaco, Phys. Rev. C **65**, 051301(R) (2002).
[16] S. Cohen and D. Kurath, Nucl. Phys. **73**, 1 (1965).
[17] B. A. Brown and W. A. Richter, Phys. Rev. C **74**, 034315 (2006).
[18] R. Machleidt, Phys. Rev. C **63**, 024001 (2001).
[19] L. Coraggio, A. Covello, A. Gargano, N. Itaco, and T. T. S. Kuo (2008), arXiv:0805.2478v1 [nucl-th].
[20] T. T. S. Kuo, S. Y. Lee, and K. F. Ratcliff, Nucl. Phys. **A176**, 65 (1971).
[21] T. T. S. Kuo, J. Shurpin, K. C. Tam, E. Osnes, and P. J. Ellis, Ann. Phys. (NY) **132**, 237 (1981).
[22] K. Suzuki and S. Y. Lee, Prog. Theor. Phys. **64**, 2091 (1980).
[23] J. Blomqvist and A. Molinari, Nucl. Phys. **A106**, 545 (1968).
[24] F. Andreozzi, Phys. Rev. C **54**, 684 (1996).
[25] G. A. Baker and J. L. Gammel, *Mathematics in Science and Engineering: The Padé Approximant in Theoretical Physics* (Academic Press, New York, 1970), Vol. 71.
[26] T. Engeland, the OSLO shell-model code 1991–2006 (unpublished).
[27] Data extracted using the NNDC On-line Data Service from the ENSDF database, file revised as of July 7, 2009.
[28] G. Audi, A. H. Wapstra, and C. Thibault, Nucl. Phys. **A729**, 337 (2003).
[29] B. H. Wildenthal, E. Newman, and R. L. Auble, Phys. Rev. C **3**, 1199 (1971).